

STIFFNESS ANALYSIS OF A CABLE-DRIVEN COORDINATELY LIFTING ROBOT

Xijie WANG¹

The dynamics and stiffness of a cable-driven coordinately lifting robot (CDCLR) system is studied in this paper. Firstly, the mechanism composition and working principle of the designed CDCLR were introduced. Secondly, the kinematics and dynamics model of the CDCLR system were established, and on this basis, a cable tension optimization method was given. The analytical expression of the stiffness for the CDCLR system was then derived. Finally, the dynamic model of CDCLR was verified, by a numerical example, and the stiffness distribution of the CDCLR system was discussed. The research results will provide a theoretical basis for the stability of the CDCLR and the motion planning control problem of the fixed pulleys.

Keywords: coordinately lifting robot, cable-driven parallel robot, dynamics, optimization method, stiffness.

1. Introduction

In recent years, the cable-driven parallel robots (CDPR) have been widely used in the fields of rehabilitation, port hoisting, ocean engineering, radio telescopes, and wind tunnel tests and so on [1-2], mainly because the workspace and stiffness of this type of robot can be adjusted, and it has high motion speed, good flexibility, strong reconfigurability and ability to complete more complex lifting tasks [3], the CDPR has attracted the interest of many engineering researchers.

Because the above-mentioned performance advantages and characteristics of the CDPR, the application research of the CDPR system in lifting and transportation aspect is of great significance. Prof. Zhao Z-g. studied a multi-robot coordinately towing robot system. The motion error of the towing robot system and the sensitivity of the error sources to the motion error of the lifted object were analyzed using the total differential method of the matrix [4], and the dynamics of the system was studied [5-6]. Liu. et al. studied the optimization problem of the cable tensions using the adaptive genetic algorithm [7]. Su. et al. proposed an optimization method of an Adaptive Multi-Island Genetic Algorithm based on Information Entropy of the Population based on the genetic algorithm. The optimization solution was carried out to analyze the cable tensions of the CDPR.

¹ Lecturer, School of Railway Locomotive, Hunan Vocational College of Railway Technology, Hunan, China, e-mail: wangxijie1929@outlook.com

The research results show that this method effectively improves the ability and practicability of global optimization solution [8].

The stiffness of the CDPR system is of great significance to the motion stability and motion accuracy of the lifted objects [9], so its stiffness problem is studied by the scientists. Ma. et al. discussed the static stiffness of the multi-robot towing robot system considering the stiffness of each robot, but the stiffness of the cables did not consider [10]. Zi. et al. derived the analytical expressions of the stiffness for the CDPR along the three coordinate axes [11]. Marc Arsenault analyzed the feasible region and stiffness of the cable parallel mechanism considering the cable quality [12]. Duan. et al. studied the stiffness of a CDPR with a spring. After adding the spring, the fixed stiffness and controllable stiffness of the system are increased [13-14], but the elasticity of the cables did not consider. Therefore, it is necessary to consider the elasticity of the cables to conduct in-depth research on the stiffness of the CDCLR system in order to reasonably plan the work task of the lifted object and improve the structure of the CDCLR.

Based on the above research work, a CDCLR is introduced in this paper. The CDCLR has three degrees of freedom. It can realize the desired motion control of the lifted object through the coordinated control of four groups of cable drive units, and its dynamics and stiffness are analyzed. The other parts of this paper are arranged as follows: the mechanism model and working principle of the CDCLR are described in detail in Section 2. In Section 3, the kinematics and dynamics models of the CDCLR are derived, and the optimization method of the cable tensions is given through the minimum variance of the cable tensions. The analytical expression of the stiffness for the CDCLR is derived in detail in Section 4. A simulation analysis is carried out through a special example in Section 5. Finally, the conclusions of this paper and future work are given.

2. Mechanical design

The desired motion control of the lifted object for the CDCLR can be realized through the coordinated movement of the cables. In the designed CDCLR in this paper, the lifted object has three degrees of freedom. The structure model of the CDCLR is shown in Fig. 1, which its mechanical system is mainly composed of motors, guide pulleys, cables, lifted object and masts.

In the CDCLR system, one end of the cables is fixed to the lifted object, and the other end is fixed to the winch mounted on the motor through the guide pulley. According to the actual requirements, the motion control plan is completed, in the control center, and the control command is generated and then sent them to the lower computer to control the motion of the motors. The motor drive cable motion to realize the elongation and contraction movement of the cable. The spatial motion of the lifted object can be realized by the coordinated motion control of the four sets of cables. The cable length displacement sensors and the

tension sensors can collect the relevant movement data of the system, and then transmit them to the control center to participate in the control calculation of the CDCLR system. The closed-loop control of the CDCLR system can be realized.

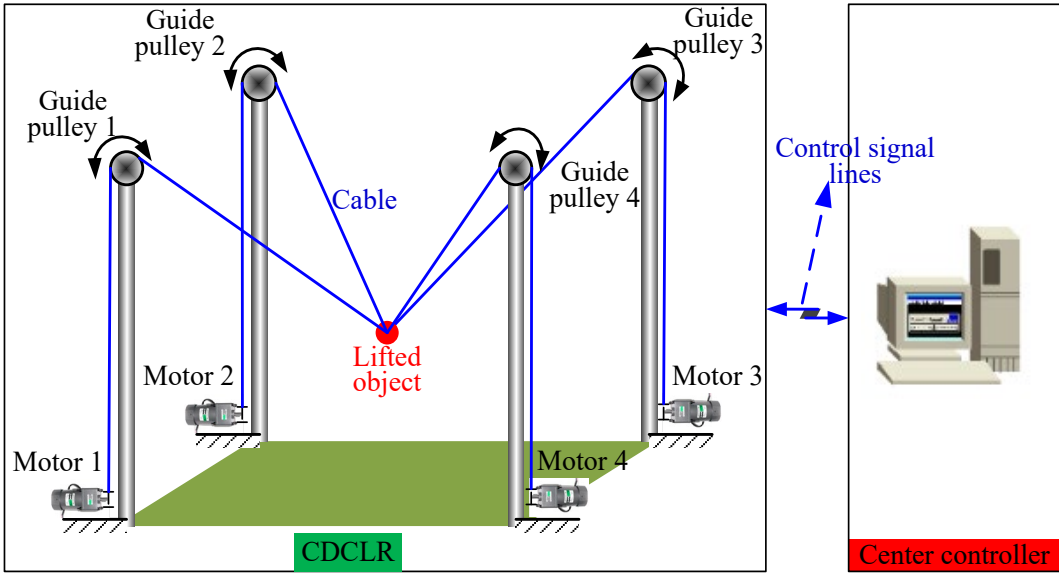


Fig. 1. The structure model of the CDCLR

In this study, it is assumed that all connection points are ideal. Due to the mass and radius of the guide pulley used are small, the friction between the cable and the guide pulley can be ignored. In addition, assuming that the cable is an ideal straight line, the mass of the cable and the deflection deformation caused by the cable mass are ignored.

3. Kinematics and dynamics analysis

The schematic diagram of the CDCLR is shown in Fig. 2. The global coordinate system $O-xyz$ is established. p_i ($i=1,2,3,4$) represents the position of the guide pulley, denoted as $p_i(x_i, y_i, z_i)$. P denotes the lifted object, denoted as $P(x, y, z)$. l_i denotes the length of the cable between the guide pulley p_i and the lifted object P , t_i represents the cable tension. mg represents the gravity of the lifted object.

The inverse kinematics problem is that when the expected position of the lifted object in the global coordinate system are given, solving the motion variables of the corresponding cables. Therefore, the inverse kinematics of the CDCLR can be expressed as:

$$l_i = \mathbf{O}p_i - \mathbf{O}P \quad (1)$$

$$l_i = \|\mathbf{O}p_i - \mathbf{O}P\| \quad (2)$$

Where \mathbf{l}_i denotes the length vector of the cables. \mathbf{Op}_i and \mathbf{OP} represent the position vector of the guide pulley p_i and the lifted object P in the global coordinate system, respectively.

The relationship between speed of the cables and the lifted object can be expressed as:

$$\dot{\mathbf{L}} = \mathbf{J}\dot{\mathbf{P}} \quad (3)$$

Where $\dot{\mathbf{L}}$ denotes the speed vector of the cable. $\dot{\mathbf{P}}$ denotes the speed of the lifted object. \mathbf{J} denotes the Jacobian matrix of the CDCLR.

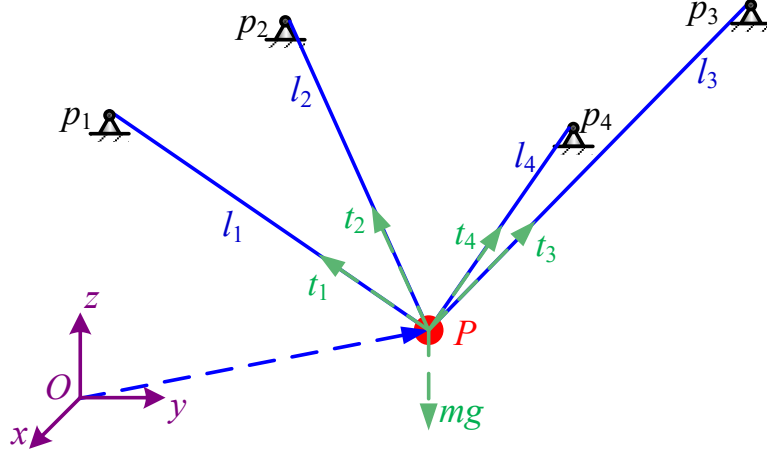


Fig. 2. Kinematic model of CDCLR for the logistics warehouse

The inverse dynamics problem of the CDCLR is that when the expected motion trajectory of the lifted object is given, solving all cable tensions. According to Newton-Euler equation, the dynamic model of the CDCLR can be obtained, which can be expressed as:

$$\sum_{i=1}^4 (t_i \mathbf{u}_i) + m\mathbf{g} = m\ddot{\mathbf{P}} \quad (4)$$

Where $\ddot{\mathbf{P}}$ denotes the acceleration of the lifted object. \mathbf{g} denotes the acceleration of gravitation. \mathbf{u}_i denotes the unit vector of the i^{th} cable, which can be specifically expressed as:

$$\mathbf{u}_i = \frac{\mathbf{Op}_i - \mathbf{OP}}{\|\mathbf{Op}_i - \mathbf{OP}\|} \quad (5)$$

The dynamical model of the CDCLR can be further organized as:

$$\mathbf{J}\mathbf{T} = \mathbf{F} \quad (6)$$

Where $\mathbf{T} = [t_1, t_2, t_3, t_4]^T$ is vector of the cable tensions. $\mathbf{F} = m\ddot{\mathbf{P}} - m\mathbf{g}$.

According to the configuration of the CDCLR, the matrix \mathbf{J} is a non-square matrix. Therefore, the cable tensions need to be solved by the pseudo-inverse of the matrix. The cable tensions can be expressed as:

$$\mathbf{T} = \mathbf{J}^+ \mathbf{F} + \boldsymbol{\alpha} \cdot \mathbf{N}(\mathbf{J}^T) \quad (7)$$

Where $\mathbf{J}^+ = \mathbf{J}^T (\mathbf{J} \mathbf{J}^T)^{-1}$ denotes the pseudo-inverse matrix of \mathbf{J} . $\boldsymbol{\alpha}$ is an arbitrary vector. $\mathbf{N}(\mathbf{J}^T)$ denotes the zero space vector of \mathbf{J} .

Taking into account the load capacity of the motor and the stability of the system, the cable tensions should meet the condition: $\mathbf{T}_{\min} \leq \mathbf{T} \leq \mathbf{T}_{\max}$. \mathbf{T}_{\min} is the pretension of the cable to prevent the pseudo-drag problem of the cables. \mathbf{T}_{\max} is the maximum allowable cable tension determined by the cable material and the load capacity of the motor, at this time, $\boldsymbol{\alpha}$ satisfies the following conditions:

$$\alpha_l = \max_{1 \leq i \leq 4} \left\{ \min_{1 \leq i \leq 4} \left(\frac{t_{\min} - t_{s,i}}{N_i(\mathbf{J}^T)}, \frac{t_{\max} - t_{s,i}}{N_i(\mathbf{J}^T)} \right) \right\} \leq \alpha \leq \alpha_h = \min_{1 \leq i \leq 4} \left\{ \max_{1 \leq i \leq 4} \left(\frac{t_{\min} - t_{s,i}}{N_i(\mathbf{J}^T)}, \frac{t_{\max} - t_{s,i}}{N_i(\mathbf{J}^T)} \right) \right\} \quad (8)$$

Where α_h and α_l represent the upper and lower bounds of α , respectively, $t_{s,i}$ is the elements of the special solution vector of equation (6).

The CDCLR is a fully constrained mechanism, and there is a problem that the cable tension is not unique. In order to meet the requirements of practical applications, it is necessary to obtain the determined value of the cable tensions in real-time. Therefore, further research on the optimization of the cable tensions is required. The change of cable tensions and the uniformity of its distribution are of great significance to the safe operation of the CDCLR. Therefore, the minimum variance of cable tensions is chosen as the optimization objective function of cable tensions in this paper. At this time, the optimization mathematical model of cable tensions can be described as:

$$\begin{cases} \min f(\alpha) = \frac{1}{4} \left[\sum_{i=1}^4 (t_i - E(t))^2 \right] \\ \text{s.t. } \mathbf{J}^T \mathbf{T} = \mathbf{F} \\ \alpha_l \leq \alpha \leq \alpha_h \end{cases} \quad (9)$$

Where $E(t)$ is the average value of cable tensions at the current moment.

The calculation diagram of optimization algorithm of the cable tensions for the CDLR is shown in Fig.3.

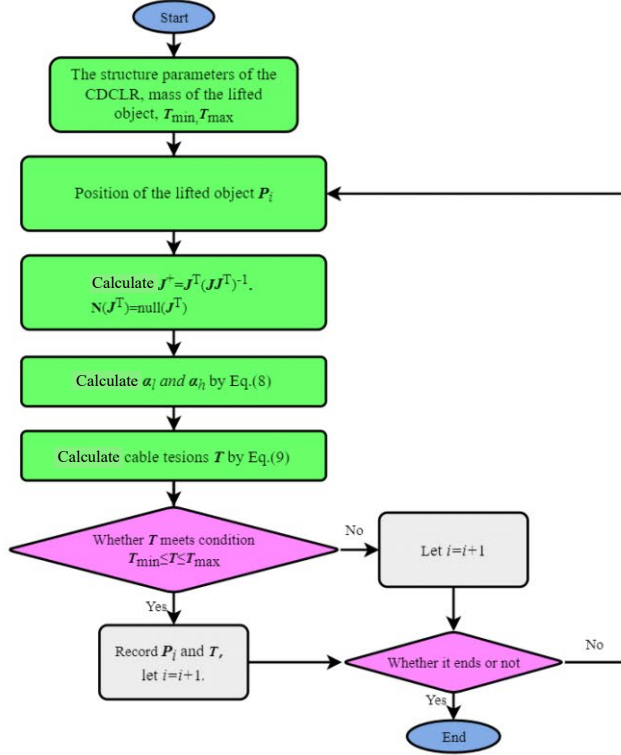


Fig. 3 Calculation diagram of optimization algorithm of the cable tensions for the CDLR

4. Stiffness analysis

The stiffness of the CDCLR mechanism refers to the amount of the applied force required to cause the change of unit displacement of the lifted object. The stiffness has a significant impact on the stability of the CDCLR system and the position accuracy of the lifted object when the interference force is acted on. The current research did not consider the elasticity of the cables. Therefore, the cable model in this paper needs to be modified before analyzing the stiffness of the CDCLR. In other words, in this study, the cables have a certain degree of elasticity, which means that when the cable is under an external force, the elastic deformation will occur.

According to the definition of mechanism stiffness, the stiffness of the CDCLR can be expressed as:

$$\mathbf{K} = \frac{\delta \mathbf{F}}{\delta \mathbf{P}} = \left(\frac{\delta \mathbf{J}}{\delta \mathbf{P}} \mathbf{T} + \mathbf{J} \frac{\delta \mathbf{T}}{\delta \mathbf{P}} \right) = \mathbf{K}_c + \mathbf{K}_f \quad (10)$$

Where the stiffness \mathbf{K} represents the relationship between the interference force $\delta \mathbf{F}$ and spatial displacement $\delta \mathbf{P}$. \mathbf{K}_c is related to the cable tension and the system structure, which can be controlled by the cable tension. Therefore, it is

called the controllable stiffness of the CDCLR. \mathbf{K}_f is related to the system structure and the position of the lifted object. Hence, it can be called the fixed stiffness of the CDCLR.

Although the fixed stiffness of the CDCLR is not controlled by the cable tension, it still has a greater impact on the system stiffness of the CDCLR. It can be seen from equation (10) that the fixed stiffness of the CDCLR can be further written as:

$$\mathbf{K}_f = \mathbf{J} \frac{\delta \mathbf{T}}{\delta \mathbf{l}} \frac{\delta \mathbf{l}}{\delta \mathbf{P}} = -\mathbf{J} \frac{\delta \mathbf{T}}{\delta \mathbf{l}} \mathbf{J}^T \quad (11)$$

Based on the cable model, one can obtain:

$$\frac{\delta t_i}{\delta l_i} = \frac{E_i A_i}{l_{i0}} \quad (12)$$

Where E_i , A_i and l_{i0} respectively represent the elastic modulus, cross-sectional area and static length of the cable.

Substituting Eq. (12) into Eq. (11) yields:

$$\mathbf{K}_f = -\mathbf{J} \cdot \text{diag}\left(\frac{E_1 A_1}{l_{10}}, \dots, \frac{E_4 A_4}{l_{40}}\right) \cdot \mathbf{J}^T \quad (13)$$

Assuming that when the position of the lifted object has a small deviation $\delta \mathbf{P}$, the unit vector of the cable changes from \mathbf{e} to \mathbf{e}' , and the length vector of the cable changes from \mathbf{l} to \mathbf{l}' , then the change of the unit vector of the cables can be derived as:

$$\delta \mathbf{e}_i = \mathbf{e}' - \mathbf{e}_i = \frac{\mathbf{l}'}{\|\mathbf{l}'\|} - \frac{\mathbf{l}}{\|\mathbf{l}\|} = \begin{bmatrix} e_{xi}^2 - 1 & e_{xi}e_{yi} & e_{xi}e_{zi} \\ e_{xi}e_{yi} & e_{yi}^2 - 1 & e_{yi}e_{zi} \\ e_{xi}e_{zi} & e_{yi}e_{zi} & e_{zi}^2 - 1 \end{bmatrix} \delta \mathbf{P} \quad (14)$$

Where $\mathbf{e}_i = [e_{xi}, e_{yi}, e_{zi}]^T$.

Therefore, the controllable stiffness of the CDCLR can be written as:

$$\mathbf{K}_c = \sum_{i=1}^4 \left(\frac{t_i}{l_i} \begin{bmatrix} e_{xi}^2 - 1 & e_{xi}e_{yi} & e_{xi}e_{zi} \\ e_{xi}e_{yi} & e_{yi}^2 - 1 & e_{yi}e_{zi} \\ e_{xi}e_{zi} & e_{yi}e_{zi} & e_{zi}^2 - 1 \end{bmatrix} \right) \quad (15)$$

Substituting Eqs. (11) and (15) into Eq. (10), one can obtain the stiffness of the CDCLR system, which can be expressed as:

$$\mathbf{K} = \sum_{i=1}^4 \left(\frac{t_i}{l_i} \begin{bmatrix} e_{xi}^2 - 1 & e_{xi}e_{yi} & e_{xi}e_{zi} \\ e_{xi}e_{yi} & e_{yi}^2 - 1 & e_{yi}e_{zi} \\ e_{xi}e_{zi} & e_{yi}e_{zi} & e_{zi}^2 - 1 \end{bmatrix} \right) - \mathbf{J} \text{diag}\left(\frac{E_1 A_1}{l_{10}}, \dots, \frac{E_4 A_4}{l_{40}}\right) \mathbf{J}^T \quad (16)$$

5. Numerical example

In order to analyze the rationality of the kinematics, dynamics and stiffness models, a numerical example is carried out with the MATLAB software for verification and analysis in this paper. The parameters of the example are shown in Table 1.

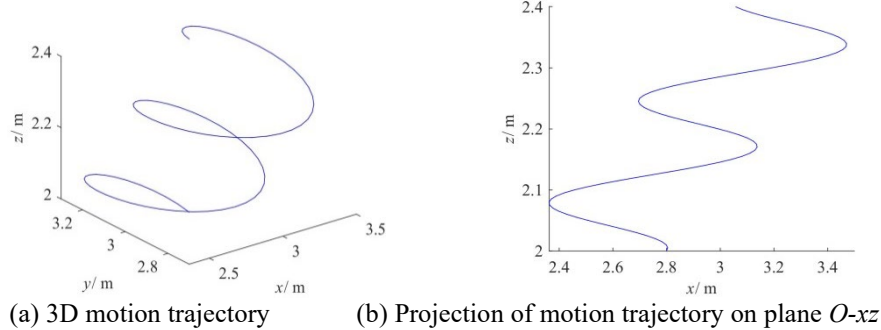
Table 1. Parameters of the CDCLR

Parameters	Value	Parameters	Value
Position of the point p_1	(10, 0, 5) m	Cross-section of cable A	2.54 mm ²
Position of the point p_2	(0, 0, 5) m	Elastic modulus of steel cable E	194.02 GPa
Position of the point p_3	(0, 10, 5) m	Tension range of cables $[t_{\min}, t_{\max}]$	[10, 3500]N
Position of the point p_4	(10, 10, 5) m	Mass of the lifted object m	30 kg

The movement trajectory shown in equation (17) is selected as the expectation of the lifted object, and the cable tensions are solved using the minimum variance optimization method. In equation (17), r is the radius of the spiral line. a is the frequency of the spiral line. b and c are the velocity at which the spiral line moves in the x and z directions, respectively. Let $r=0.3$, $a=0.3$, $b=0.1$, $c=0.05$, $(x_0, y_0, z_0)=(2.5, 3, 2)$ m. The expectation of the lifted object can be written as:

$$\begin{cases} x = r \cos(2a\pi t) + bt + x_0 \\ y = r \sin(2a\pi t) + y_0 \\ z = ct + z_0 \end{cases} \quad (17)$$

According to the above parameters and dynamical equation, the obtained trajectory of the lifted object and the optimized cable tensions are shown in Fig. 4. It can be seen that the trajectory of the lifted object is a spiral inclined in the positive x direction. The corresponding change of the cable tensions is smoothly, which has a positive meaning for the stability of the lifted object during the movement.



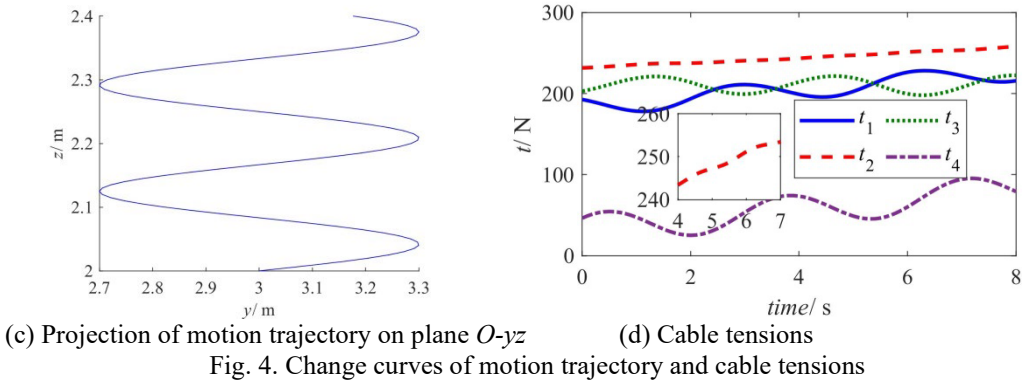


Fig. 4. Change curves of motion trajectory and cable tensions

When the position of the lifted object is (5, 4, 2.5) m, the cable tensions are $\mathbf{T} = [242.51, 242.51, 192.88, 192.88]\text{N}$ calculated by the dynamical model and optimization algorithm. The fixed stiffness matrix, controllable stiffness matrix and system stiffness matrix of the CDCLR are as follows:

$$\mathbf{K}_f = 10^8 \times \begin{bmatrix} 1.208 & 0 & 0 \\ 0 & 1.131 & -0.0355 \\ 0 & -0.0355 & 0.3019 \end{bmatrix}$$

$$\mathbf{K}_c = \begin{bmatrix} -62.780 & 1.243 \times 10^{-14} & -6.217 \times 10^{-15} \\ 1.243 \times 10^{-14} & 68.525 & -4.441 \\ -6.217 \times 10^{-15} & -4.441 & -103.895 \end{bmatrix}$$

$$\mathbf{K} = 10^8 \times \begin{bmatrix} 1.208 & 1.243 \times 10^{-22} & -6.217 \times 10^{-23} \\ 1.243 \times 10^{-22} & 1.131 & -3.55 \times 10^{-2} \\ -6.217 \times 10^{-23} & -3.55 \times 10^{-2} & 0.3019 \end{bmatrix}$$

The expression and calculation results of the fixed stiffness \mathbf{K}_f show that the fixed stiffness matrix is a symmetric matrix. The controllable stiffness is significantly smaller than the fixed stiffness, which indicates that the stiffness of the driving motion branch chain has a greater impact on the stiffness of the CDCLR system. The diagonal elements $\mathbf{K}(1, 1)$, $\mathbf{K}(2, 2)$ and $\mathbf{K}(3, 3)$ in the system stiffness matrix \mathbf{K} represent the stiffness \mathbf{K}_x , \mathbf{K}_y and \mathbf{K}_z of the robot along the x , y and z axes, respectively. In addition, other elements in the matrix \mathbf{K} characterize the coupling stiffness of the mechanism in the corresponding direction. It can be seen from the calculation results that the absolute values of diagonal elements $\mathbf{K}(1, 1)$, $\mathbf{K}(2, 2)$ and $\mathbf{K}(3, 3)$ decrease in order, which shows that when the lifted object is at the position (5, 4, 2.5)m, the stiffness of movement along the x direction is the largest, and the stiffness of movement along the z direction is the smallest.

In order to further analyze the stiffness of the CDCLR system in the entire workspace, combined with the structure scheme of the CDCLR system and

structural parameters, the stiffness value K_x , K_y and K_z of the CDCLR system along the x , y and z axes were calculated, respectively. The distributions in different sections are shown in Fig. 5-6.

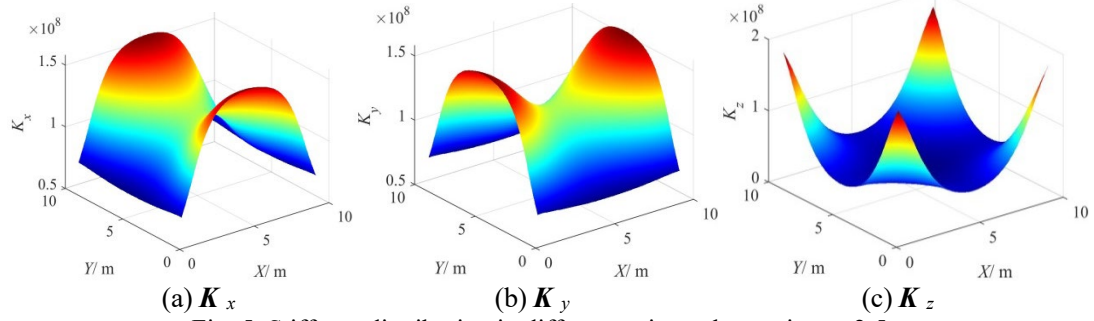


Fig. 5. Stiffness distribution in different axis on the section $x=2.5\text{m}$

When the lifted object moves in the horizontal section $x=2.5\text{ m}$, the stiffness distribution in different directions is shown in Fig. 5. In the horizontal section, K_x , K_y and K_z are all symmetrically distributed about the center line of the section, and there is an inverse growth phenomenon in the boundary area of the section, which is caused by the correction of the cable tensions in the boundary area. On the whole, the stiffness value K_x is the largest and the stiffness value K_z is the smallest. In Fig. 6(c), the stiffness value K_z is obviously increased near the guide pulleys. This is caused by correcting the cable tension through the optimization algorithm to prevent the pseudo-drag of the cables.

When the lifted object moves in the vertical section $y=5\text{ m}$, the stiffness distribution in different directions is shown in Fig. 6. In the vertical section, K_x , K_y and K_z are all symmetrically distributed about the straight line $x=5\text{ m}$. On the whole, the stiffness value K_x is the largest and the stiffness value K_z is the smallest. In Fig. 6(a) and (b), both K_x and K_y gradually increase as increase of the value z , and K_z gradually decreases as increase of the value z . Because the structure of the CDCLR is symmetrically distributed, the stiffness distribution in the x -vertical section is the same as the stiffness distribution in the y -vertical section, so this paper will not repeat it.

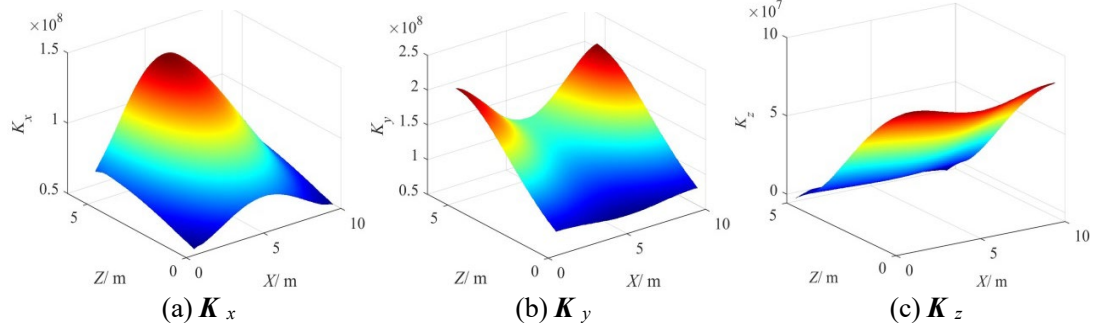


Fig. 6. Stiffness distribution in different axis on the section $y=5\text{m}$

In summary, it can be seen that the overall stiffness of the CDCLR system is larger in the upper and central areas of the workspace than in the lower and boundary areas, which means that when the lifted object moves in the upper and central areas of the workspace, the stability and positioning accuracy of the system are better. Therefore, in practical applications, the height of the guide pulleys can be appropriately reduced to improve its stability and positioning accuracy based on actual needs and on the basis of meeting the motion planning of the lifted object.

6. Conclusions

A CDCLR is introduced in this paper, and the dynamics and system stiffness of the CDCLR are studied. The research results show that in the workspace, the stiffness of the CDCLR system is larger in the upper and center areas of the workspace than in the lower and boundary areas. In addition, at the same position, the stiffness of the CDCLR system in the x -direction is the largest, and the stiffness of the CDCLR in the z -direction is smallest. The research results provide a basis for further research on key issues such as the stability of the CDCLR system and impedance control strategy. For example, when the expected trajectory of motion is given, the change law of cables lengths and cable tensions will be obtained by the kinematic and dynamic models of the CDCLR system, and a double closed-loop impedance controller that meets certain compliance performance will be then designed in combination with the system stiffness model.

Acknowledgement

This work is supported by Scientific Research Project of Department of Education of Hunan Province, China (Grant No. 21C1319) and Vocational Education Highland Construction Theory and Practice Research Project of Hunan Province, China (Grant No.ZJGD2021087). The author wishes to thank its generous financial assistance.

R E F E R E N C E S

- [1] *H. Wei, Y. Qiu, J. Yang.* “An Approach to Evaluate Stability for Cable-based Parallel Camera Robots with Hybrid Tension-stiffness Properties”. International Journal of Advanced Robotic Systems, **vol.12, no.185**, 2015, pp.1-12.
- [2] *Z. Zhao, Y. Wang, C. Su, et al.* “Analysis and Optimization on Inverse Kinematics for Multi-Robot Parallel Lifting Systems”. Applied Mathematics and Mechanics, **vol.38, no.6**, 2017, pp.643-651.
- [3] *Y. L. Wang, K.Y. Wang, K.C. Wang, et al.* “Safety Evaluation and Experimental Study of a New Bionic Muscle Cable-Driven Lower Limb Rehabilitation Robot”. Sensors, **vol.20, no.24**, 2020, pp.7020.
- [4] *Y. Wang, Z. Zhao, G. Shi, et al.* “Dynamics analysis of the cable-tying close-coupling multi-robot collaboratively towing system”. UPB Scientific Bulletin, Series D: Mechanical

Engineering, **vol.79, no.2**, 2017, pp.3-20.

- [5] *Y. Ma, Z.g. Zhao, Y.l. Wang, et al.* “Analysis of Feasible Region on the Multi Robot Combined Lifting System by Considering the Static Stiffness”. Computer Simulation, **vol.34, no.7**, 2017, pp.307-311.
- [6] *Y. Wang, Z. Zhao, G. Shi, et al.* “Analysis of workspace of cable-typing close-coupling multi-robot collaboratively towing system”. UPB Scientific Bulletin, Series D: Mechanical Engineering, **vol.78, no.4**, 2016, pp.3-14.
- [7] *Y. L. Wang, K.Y. Wang, X. Li, et al.* “Control Strategy and Experimental Research of Cable-Driven Lower Limb Rehabilitation Robot”. IEEE Access, **vol.9**, 2021, pp.79182-79195.
- [8] *Y. Su, Y. Y. Qiu, H. L. Wei.* “Dynamic modeling and tension optimal distribution of cable-driven parallel robots considering cable mass and inertia force effects,” Eng. Mech. **vol.33, no.11**, 2016, pp.231-239 + 248.
- [9] *Y. L. Wang, K.Y. Wang, Y.J. Chai, et al.* “Research on Mechanical Optimization Methods of Cable-Driven Lower Limb Rehabilitation Training Robot”. Robotica, **vol.41, no.1**, 2022, pp.154-169.
- [10] *Z. Zhao, Y. Wang, C. Su, et al.* “Analysis of the workspace and dynamic stability of a Multi-Robot Collaboratively Towing Systems”. Journal of Vibration and Shock, **vol.36, no.16**, 2017, pp.44-50.
- [11] *Carricato M, Merlet J P.* Geometrico-Static Analysis of Under-Constrained Cable-Driven Parallel Robots. Advances in Robot Kinematics, **vol.12**, 2012, pp.269-285.
- [12] *Carricato M, Merlet J P, Waters T P.* “Stability analysis of underconstrained cable-driven parallel robots”. IEEE Transactions on Robotics, **vol.1, no.29**, 2013, pp.288-296.
- [13] *P. M. Bosscher, E.-U. Imme.* A stability measure for under-constrained cable-driven robots, IEEE International Conference on Robotics and Automation 2004, Proceedings of ICRA, New Orleans, LA, USA, 2004.
- [14] *S. Behzadipour, A. Khajepour.* “Stiffness of cable-based parallel manipulators with application to stability analysis”. J. Mech. Des., **vol.128, no.1**, 2006, pp. 303-310.